

## CHAPTER IV

### PREPARATION AND CHARACTERIZATION OF VERY FINE ELECTROSPUN POLYACRYLONITRILE FIBERS AS A PRECURSOR FOR CARBON FIBERS

Jutawan Sutasinpromprae, Pitt Supaphol\* and Manit Nitithanakul

The Petroleum and Petrochemical College, Chulalongkorn University, Bangkok 10330,  
Thailand

#### ABSTRACT

Carbon fiber is one of the strongest materials which is useful in many fields such as composite materials. To prevent delaminating problem of the composite, reducing the carbon fiber size could be a way to solve the problem. Among the methods for producing very small fibers, electrospinning process could be the most appropriate one. This is because electrospinning is a straightforward, cost effective method which can produce very fine fibers with the diameter ranging from a few micrometers to nanometers. To produce the smallest carbon fibers, a commercial polyacrylonitrile (PAN) was used. The effects of processing parameters were studied including polymer concentration, applied voltage, collection distance nozzle radius, polarity of attached electrode and take up speed. In addition, thermal properties of PAN electrospun fibers were investigated and compared with that of conventional PAN fiber.

(**Key words:** polyacrylonitrile, electrospinning, carbon fiber, processing parameters, thermal study)

- 
- To whom correspondence should be addressed: Fax: +66-2215-4459; E-mail address: [Pitt.s@Chula.ac.th](mailto:Pitt.s@Chula.ac.th)

## 1. INTRODUCTION

Carbon fibers are the primary reinforcement used to increase the stiffness and strength of lightweight advanced composites commonly used in aerospace, recreation, and industrial applications [1]. Among the various carbon fiber precursors, polyacrylonitrile (PAN) has wide acceptability due to the high carbon yield and flexibility for tailoring of the structure of the final product [2]. Therefore, most (90%) of carbon fiber produced worldwide are obtained from PAN [3]. However, it is generally accepted that a major limitation to the tensile strength of polyacrylonitrile-based carbon fibers is the presence of surface defect and large fiber diameter [4].

Recently, there has been a trend towards thinning precursor fibers to obtain carbon fibers with small diameter (4.5-5.0  $\mu\text{m}$  compared to the 7-8  $\mu\text{m}$  diameter usually obtained) to provide uniformity of thermal stabilization in very short time.[4]. Electrospinning process can be used to produce carbon fibers with intention of attenuating fiber diameter to promote more uniform heat treatment, increasing molecular orientation to promote modulus and avoiding skin-core morphology.

Electrospinning is a process using electrical field as a driving force to create electrically charged jet of polymer solution or melt, which dries or solidifies to leave a polymer fiber. This process provides high molecular orientation fiber [5, 6, 7] in non-woven form with diameter ranging from microscale to nanoscale. In addition, the non-woven fibers possess high surface to mass ratio with very small pore sizes that are useful in filter, catalyst supporter in high temperature reactions, in composite to improve mechanical properties and for thermal management in semiconductor device as well [8].

In 1971, Baumgarten [9] produced acrylic microfibers from the solution of poly (acrylonitrile-co-methylacrylate)(PAN) and observed the relationship between fiber diameter, jet length, surrounding gas, solution viscosity, and solution feed rate. He found that diameter increased approximately as the 0.5 power of solution viscosity but flow rate has a small effect on fiber diameter. Nevertheless, he did not characterize the molecular structure of the fiber.

Chun *et al* (1999) [8] already produced electrospun PAN nanofibers, which have diameter from 100 to 500 nm, from the solution of special acrylic fiber (SAF) by varying the voltage and the distance between a nozzle and collector (collection distance). They converted electrospun PAN nanofibers to carbon nanofibers by heating at 270°C in air for 15 minutes followed by heating at 800°C in inert atmosphere for 1 h. However, they did not report the difference in thermal behavior of PAN electrospun fibers compared with PAN.

Two years later, MacDiarmid *et al.* (2001) [10] used similar technique to Chun's work to produce carbon nanofibers from electrospun PAN fiber by first heating at 200°C in air for 20 minutes followed by heating at 800°C for 2 h under nitrogen. They also studied the conductivity of a 600-nm diameter carbon fiber.

This work focused on the effect of processing parameter affecting the morphology i.e. the fiber diameter, the density of bead, fiber alignment. Moreover, the thermal behaviour of electrospun fibers was compared with the conventional PAN fiber by using Differential Scanning Calorimetry (DSC). A commercial grade PAN-co-methylacrylate was chosen to study because it is cheap and readily available and easy to find.

## 2. EXPERIMENTAL DETAILS

### 2.1. Materials

Commercial grade PAN fibers with molecular weight of 55,500 g mol<sup>-1</sup> were used to prepare PAN solution. It composed of 91.4% acrylonitrile monomer (CH<sub>2</sub>=CHCN) and 8.6% methylacrylate monomer (MA, CH<sub>2</sub>=CHCOOHCH<sub>3</sub>). 99.98%wt. of dimethylformamide (DMF) was used as the solvent. PAN nanofibers, which produced from these PAN solutions, were later used as precursors for producing carbon nanofibers.

## 2.2. Sample Preparation and Solution Properties Measurement

PAN solution in DMF was prepared at the concentration of 2.1 to 17.4 percentage by weight (wt%). The viscosity of PAN solutions was determined at 30°C by using a Brookfield digital viscometer (model LVTDCP). A tensiometer (Krüss model KS10T) was used to measure the surface tension of the solutions. The conductivity of PAN solution was measured as well by using conductometer.

## 2.3. Experimental Set-up

The experimental set-up [11] for studying the effect of processing parameters on electrospun fibers morphology was as shown in Figure 1. PAN solution was placed in a 50-mL glass syringe. The syringe was clamped with an insulator stand at approximately -10° from horizontal. It was placed at 15 cm from the grounded stationary collection screen. The polymer solution was subjected to external electrical field by attaching positive electrode to the nozzle. The constant pressure of nitrogen gas was applied into the syringe to suspend the polymer drop at the tip of the nozzle. The pressure was increased when polymer concentration increased to achieve similar suspending polymer drop. The electrospun fibers were kept in vacuum for 24-h prior to characterization to ensure complete drying of the sample. In case of studying the effect of take-up speed, an adjustable speeds rotating drum was used as a collector.

## 2.4. Characterization of PAN Precursors by FTIR

Infrared spectroscopy (FTIR) was performed on commercial PAN precursor fibers to determine their composition (particularly comonomer types) and study the changes of chemical structure of stabilized and carbonized electrospun PAN fibers. FTIR measurements were made on a Bruker Model 106/S Fourier transform infrared spectrometer using resolution of  $\pm 4 \text{ cm}^{-1}$  and 16 scans per sample. Infrared spectra were recorded in the wavenumber ranging from 400-4000  $\text{cm}^{-1}$ .

Thin films of PAN were prepared by casting from 15.9 wt% solution of PAN precursor fibers in dimethyl sulfoxide (DMSO) onto clean glass substrates followed by

drying at 30°C. The electrospun stabilised and carbonised PAN fibers were analysed in the original non-woven form.

### **2.5. Experimental Condition for Studying the Effects of Processing Parameters**

The processing conditions for studying each parameter used the same set-up as mentioned previously. The conditions for studying each parameter are shown in Table 1.

### **2.6. Continuous Stabilization and Carbonization**

A Carbolite furnace (type STF 15/75/450, maximum temperature of 1500°C) was used to convert electrospun precursors into carbon fibers. In stabilization step, the electrospun PAN fibers were heated at the temperature of 230°C at a heating rate of 1°C/min and 4L/min of purified air under tension for 5 h [4]. Consequently, the stabilised fibers were treated at the temperature of 1000°C at the same heating rate and gas flow rate under high purity nitrogen atmosphere.

### **2.7. Fiber Morphology Observation**

A JEOL 520-2AE scanning electron microscope (SEM) was used to observe the surface morphology and diameter of as-received electrospun fibers obtained, both the stabilized and carbonized PAN electrospun fibers.

### **2.8. Crystallinity Measurement**

An X-ray diffraction spectrometer (Rigaku RINT DMAX/2002H, 40 kV, 30 mA) with a  $\text{CuK}\alpha$  ( $\lambda=1.54 \text{ \AA}$ ) was used to observed the crystallinity of PAN fibers, as-received electrospun PAN, and pyrolysed electrospun PAN fibers. To confirm the effect of electrospinning process on the crystallinity of obtained fibers, the electrospun fibers were also examined by DSC.

### 3. RESULTS AND DISCUSSION

#### 3.1. PAN Fiber Composition

The FTIR spectra of cast film of conventional PAN (PAN) was shown in Figure 2. The characteristic peak of PAN at  $2243\text{ cm}^{-1}$  is due to nitrile stretching, indicating that PAN precursors contains polyacrylonitrile [4]. The peak at  $1735\text{ cm}^{-1}$  was assigned to carbonyl stretch and confirms that the presence of acid comonomer. It was probably methylacrylate ( $\text{CH}_2=\text{CHCOOCH}_3$ ) as informed by the supplier.

#### 3.2. Relations of Fiber Morphology and Solution Properties

The products obtained from the concentrations of 2.1 wt% to 17.4 wt% are shown in Figure 3(a-l). Fibers cannot be produced below concentration of 2.1 wt% and viscosity of ca.4.4 poise. The obtained product is only a fine polymeric droplet (see Figure 3 (a)). This phenomenon generally occurs in the electrospaying which a low molecular weight liquid is driven by electrical force [16], hence, entanglement between polymer chains is not high enough to form fiber. Fiber formation began at 4.0 wt% with viscosity of ca.13.6 poise while Baumgarten [9] mentioned that it started with a 7.5 wt% and 1.7 poise when the same type of copolymer was used.

There are many efforts in trying to explain about the formation of bead in electrospun fibers. For instance, Fong et al. (1999) proposed that the capillary breakup of the electrospinning jet by surface tension is the cause of the formation of beaded nanofibers [12]. Moreover, the key factors were solution viscosity, net charge carried density by the electrospinning jet. The surface tension and the solution viscosity of prepared PAN solution (see figure 4) increased when the concentration of PAN solution increased.

Therefore, when the concentration of PAN solution increased, the bead density should be increased as well. Surprisingly, SEM micrographs (see figure 3(a-l)) indicated that bead density decreased from 90 to 6 beads per  $70,000\text{ }\mu\text{m}^2$  when concentration increased from 7.8 to 11.2 wt%. Thus, there should be other parameters, which will overcome the role of surface tension and viscosity in the contraction of

charged jet.

The other cause of the bead formation should be the inhomogeneity of charge through the charged jet. At the position of the jet that has no charge, there is no electrical force to draw the jet, subsequently, surface tension and viscosity will draw back the jet and bead will be formed. If the conductivity of the jet is high enough to distribute charge throughout the jet, the beaded nanofiber would not occur. Therefore, it was hypothesized that solution conductivity should be a candidate in this case. This is because the jet with high concentration and conductivity (see Figure 5) could distribute the charge through the jet better than that with low conductivity.

Considering the diameter of electrospun fiber, it increased with increasing concentration of PAN solution (see Figure 6). This could be explained in terms of the viscosity and concentration of the solution. The higher viscosity solution, the higher viscoelastic force to restrain drawing. Thus the fiber diameter increased with increasing in PAN concentration.

On the other hand, the conductivity of solution can affect the fiber diameter as well. A jet with high conductivity should be charged up easier than the one possessing low conductivity. The more charge uptake, the more flow rate of the jet causing larger fiber diameter.

### **3.3. Effect of Collection Distance**

It was found that when the collection distance increased, the fiber diameter decreased (see Figure 7) while the collected area of electrospun PAN fiber increased (see Figure 8). The evidences from the work of Reneker *et al.* (2000) [13] could explain these results. They obtained a set of stereographic images of an electrically driven bending instability, taking place near the vertex of the envelope cone by using electronic camera. It indicated that, after a smooth segment of the jet that was straight, an array of bends suddenly developed. Then the segment of the jet in each bend elongated and the array of bends became a series of spiraling loops with growing diameters. As the perimeter of the loops increased, the cross-sectional diameter of the jet forming the loop

grew smaller. Therefore, electrospun PAN fiber collected at longer collection distance should have smaller diameter and a wider collected area.

### **3.4. Effect of Applied Voltage**

Fiber diameter increased with increasing applied voltage (see Figure 9). Due to the charge transport, electrospinning current increased, consequently, mass flow rate of polymer jet increased and fiber diameter increased as well [7]. When the other parameters (i.e., solution conductivity, concentration of PAN solution, collection distance, and flow rate) are constant.

SEM micrographs (Figure 10) indicated that the bead density is high when high electrical field was applied. The result could be explained in terms of viscoelastic properties of PAN solution. Since PAN solution is a viscoelastic fluid, when high electrical field was applied, shear rate increased [14]. The molecules have less time to undergo translation so the viscosity decreased and elastic behavior dominated. Subsequently, the jet was contracted by elastic force and beads were formed.

### **3.5. Effect of Electrode Polarity**

Figure 11 shows that the polarities of subjected electrode have no effect on fiber diameter, which is consistent with Doshi's work (1995) [15]

### **3.6. Fiber Alignment of Various Take-up Speeds**

The alignment of electrospun fibers was improved when adjustable-speed rotational collector was used (Figure 13(a-e)). In addition, the fiber diameter decreased ca. 25 % when take-up speed increased from 0 to 2500 rpm (see Figure 13).

The molecular orientation should be increased as well, leading to, the improvement in mechanical properties that should be useful for composite application. Moreover, in stabilization step of carbon fibers manufacturing, the ladder structure should be easily formed. They would be reported in further studies.

### 3.7. Effect of Nozzle Radius

When the nozzle size increased, the fiber diameter dramatically decreased (see Figure 14). It could be explained in terms of solution suspending at the end of the syringe needle. When the large size of syringe needle was used, the microdripping jet appeared where the jet originated from the bottom of a drop whose diameter is larger than the capillary diameter [16]. In addition, the larger size of nozzle should have more contact area between solution and nozzle causing more charge generating. The more of the charges, the more force to draw the solution coming out from the nozzle, as a consequent, the fiber diameter will be larger.

In case of bead density, when the nozzle radius was larger, the polymer beads tend to decrease and little beads were observed when using the 0.51 mm-nozzle (see Figure 15). It could be because of the dripping of the solution during the spinning process. When the nozzle with large radius was used, the dripping always occurred and disturbed the spinning process. The gravity force would contact the jet and bead would be formed.

### 3.8. Heat Treatment of Electrospun PAN

#### 3.8.1 FTIR Analysis

FTIR spectra of stabilized and carbonized electrospun PAN were compared to the spectra of DMSO cast film of PAN in Figure 16.

As was reported in the previous paper [17], when electrospun PAN fiber was heated in the stabilization step, the most prominent changes observed are the decrease in the intensities of the  $C\equiv N$  peak for saturated nitrile at  $2243\text{ cm}^{-1}$  and those for aliphatic C–H ones around  $2900$  and  $1450\text{ cm}^{-1}$ . Moreover, the growth of the C=N, C=O, and cyclic C=O peaks between  $1580$  and  $1700\text{ cm}^{-1}$  was observed as well. The peak at  $1372\text{ cm}^{-1}$  is due to C–H in-plane deformation and  $805\text{ cm}^{-1}$  due to out-of-plane deformation [2].

In addition, the fairly intense peak at  $1740\text{ cm}^{-1}$  for cast film of PAN, which was assigned to the C=O peak for methylacrylate, also decreased as the stabilization

proceeded. Thus the changes in the chemical structure of electrospun PAN fiber during heat treatment are the same as those in conventional PAN.

Finally, FTIR spectrum of carbonized electrospun PAN fiber did not show any peak. It meant that all functional groups were eliminated leaving a structure the same as of graphite fiber [2].

### 3.8.2 XRD Analysis

According to previous results, PAN fiber with linear chains have two major peaks at  $2\theta=17^\circ$  corresponding to (100) planes, and a minor one at  $2\theta=29^\circ$  corresponding to (101) plane [3].

The electrospun PAN fibers have only broad crystalline peak at  $2\theta=17^\circ$ , while the one of cast film of PAN shows the two major peaks mentioned in previous papers. It indicated that the crystallinity of the former was lower than the later (see Figure 17(a, b)). Thus, the electrospinning process reduced the crystallinity of PAN fiber. It is due to the molecular fracture during the spinning of the jet with very high speed close to the velocity of sound in air [9].

Considering the X-ray peaks of stabilized PAN precursors, both of the intense peak at  $2\theta=17^\circ$  and a small peak at  $2\theta=29^\circ$  are observed with the intensity quite similarly to those of the PAN (see Figure 17(c)). It was remarkable that the intense peak at  $2\theta=9.22^\circ$  (d-spacing of 0.94 nm) which have not been mentioned before was observed. It might be a space between ladder structure.

The carbonized electrospun PAN fiber has a very broad peak at around  $2\theta=24.26^\circ$  (0.36 nm) (see Figure 17(d)). This value is close to the space between the layer planes of graphite crystal at  $2\theta=26.54^\circ$  (0.3354 nm) in c-direction [2]. It indicated that carbonized electrospun PAN fiber obtained is a carbon fiber.

### 3.8.3 DSC Analysis

DSC thermograms of conventional PAN fiber and electrospun PAN fibers are compared in figure 18. The cross-linking peak of conventional PAN fiber is broader

than the one of electrospun PAN fibers.  $\Delta H$  of PAN and electrospun PAN fibers are ca.-914.876 and -787.775 J/g, respectively. It means that heat transfer of electrospun fibers, which have smaller diameter, is better than the PAN precursor tow.

The cross-linking temperature of electrospun PAN fibers, where the polymer chain form a ladder structure, is 299.5°C (onset of ca.286.6°C), which is slightly lower than PAN (308.2, onset 293.0 C). Since stabilization reaction was faster in electrospun PAN fibers than conventional PAN fiber, therefore, electrospun PAN fiber required less energy than conventional PAN fiber.

#### **3.8.4 TGA Analysis**

TGA thermograms (see Figure 19 and 20) are used to confirm that stabilization of electrospun PAN fibers (340°C) started before conventional PAN fiber (ca.345°C)

#### **3.8.5 Carbon nanofiber**

Figure 21 showed carbon fibers converted from electrospun PAN fibers (diameter of 520 nm) produced from 14.4 wt% PAN solution with the 20 kV at the collection distance of 15 cm. It possessed a diameter of ca.250 nm which is smaller than the carbon fibers obtained from previous work [8].

### **4. CONCLUSIONS**

The PAN electrospun fibers obtained from this work have a diameter ranging from ca. 69 to 730 nm. The parameters that affect the fiber morphology are solution properties including concentration, surface tension, viscosity and conductivity. To reduce the fiber diameter, applied voltage and nozzle radius should be reduced while take-off speed and collection distance should be increased. The fiber alignment could be improved by increasing the take-up speed of rotational collector. The chemical reaction during heat treatment of electrospun PAN was similar to the conventional PAN fiber. However, since stabilization reaction was faster in electrospun PAN fiber than in conventional one, it required lower energy than conventional PAN fiber. The carbon

fibers obtained have diameter of ca. 250 nm.

## ACKNOWLEDGEMENTS

The author would like to express her sincere thanks to all instructors who have taught the invaluable knowledge to her especially Asst. Prof. Pitt Supaphol and Dr. Manit Nitithanakul, her advisors, who always advised and provided suggestions throughout this work. This thesis work is partially funded by Postgraduate Education and Research Programs in Petroleum and Petrochemical Technology (PPT Consortium).

## REFERENCES

- [1] Venner, J.G., in Kroschwitz, J.I. exec. ed. and Howe-Grant, M. ed. "Kirk-othmer Encyclopedia of Chemical Technology", Vol 5, 4<sup>th</sup> ed. John Wiley, New York, p 1
- [2] Gupta AK, Paiwal DK and Bajat P, *J Macromol Sci-Rev Macromol Chem Phys*, 1991, C31, 1.
- [3] Sánchez-Soto PJ, Avilés MA, del Río JC, Ginés JM, Pascual J and Pérez-Rodríguez, *J Anal Appl Pyrolysis*, 2001, 58-59, 155.
- [4] Chen JC and Harrison IR, *Carbon*, 2002, 40, 25.
- [5] Zong X, Kim K, Fang D, Ran S, Hsiao BS and Chu B, *Polymer*, 2002, 43, 4403.
- [6] Lorrando L, John Manley R, *J Polm Sci, Polym Phys Ed*, 1981, 19, 909.
- [7] Deitzel JM, Kleinmeyer J, Harris D, Beck Tan NC, *Polymer*, 2001, 42.
- [8] Chun I, Reneker DH, Fong H, Fang X, Deitzel J, Tan NB and Kearns K, *J Adv Mat*, 1999, 311, 36.
- [9] Baumgarten PK, *J of Colloid and Interface Science* 1971, 36,1.
- [10] MacDiarmid AG, Jones WE, Norris ID, Gao J, Johnson AT, Jr, Pinto NJ, Hone J, Han B, Ko FK, Okuzaki H, Llaguno M, *Synthetic Matals*, 2001, 119, 27.
- [11] Norris ID, Shaker MM, Ko FK and MacDiarmid AG, *Synthetic metals*, 2000, 114, 110.
- [12] Fong H, Chun I, Reneker DH, *Polymer* 1999, 40.
- [13] Reneker DH, Yarin AL, Fong H and Koombhongse S, *J Appl Phys*, 2000, 87,

4531.

- [14] Alger, MSM, Polymer Dictionary, elsevier applied science, 1990, 512.
- [15] Doshi K and Reneker DH, J Electrostatics, 1995, 35, 151.
- [16] Da-Ren C, David YHP, Stanley LK, J Aerosol Sci, 1995, 26, 963.
- [17] Usam T, Iton T, Ohtani H, Tsuge S, Macromolecules, 1990, 23, 2460.

### CAPTIONS OF FIGURES

- Figure 1. Schematic diagram of experimental set up of electrospinning process.
- Figure 2. FTIR spectrum of DMSO cast film of PAN fiber.
- Figure 3. SEM micrographs of obtained electrospun PAN at various concentrations (2.1-17.4%wt).
- Figure 4. Viscosity (●) and surface tension (▼) of PAN solution in DMF as a function of concentration.
- Figure 5. Conductivity of PAN solution in DMF at concentration of 2.1 to 17.4 %wt.
- Figure 6. Concentration dependence on fiber diameter obtained by electrospinning process at collection distance of 15 cm and applied -20kv.
- Figure 7. The effect of collection distance on fiber diameter.
- Figure 8. Photographs of electrospun PAN fibers collected at various collection distances.
- Figure 9. The average of fiber diameter as function of applied voltage per unit distance.
- Figure 10 SEM micrographs of obtained PAN electrospun fibers at various applied voltages (10-30kV) collected at the collection distance of 30 cm.
- Figure 11 Influence of electrode polarity on diameter of electrospun PAN obtained from 14.4 wt% PAN solutions, which subjected by 20 kV and collected on the collection distance of 15 cm.
- Figure 12 Effect of take-up speed on fiber diameter when the adjustable speed rotational drum was used as a collector.
- Figure 13 Comparison of fiber alignment at different take-up speed of the adjustable speed rotational drum.
- Figure 14 The average diameter of electrospun fibers obtained by using various needle radius.
- Figure 15 SEM micrographs of PAN electrospun fibers when various sizes of needle radius were used.
- Figure 16 FTIR spectra of cast film of PAN (a), stabilized electrospun PAN fibers (b) and (c) carbonized electrospun PAN fibers.
- Figure 17 WAXD patterns of (a) DMSO cast film of PAN fibers, (b) electrospun PAN fibers, (c) stabilized electrospun PAN fibers, and (d) carbonized electrospun PAN fibers.

- Figure 18 DSC thermograms of (a) conventional PAN fibers and (b) electrospun PAN fibers.
- Figure 19 TGA thermogram of electrospun PAN fibers.
- Figure 20 TGA thermogram of conventional PAN fibers.
- Figure 21 SEM micrograph of carbon nanofibers converted from electrospun PAN fibers produced from 14.4 wt% PAN solution which subjected to 20 kV and at the collection distance of 15 cm.

**Table 1** The conditions for studying the effect of processing parameters.

Parameter	Polymer concentration (wt%)	Collection distance (cm)	Applied voltage (kV)	Electrode polarity	Take-up speed (rpm)	Nozzle radius (mm)
Polymer concentration	2.1-17.4	15	20	+	0	0.47
Collection distance	9.5	10-30	30	+	0,2000	0.47
Applied voltage	9.5	15	10-30	+	0	0.47
Electrode polarity	2.1-17.4	15	20	+,-	0	0.47
Take-up speed	14.4	10	20	+	0-2500	0.47
Nozzle radius	9.5	15	15	+	0	0.47-0.81

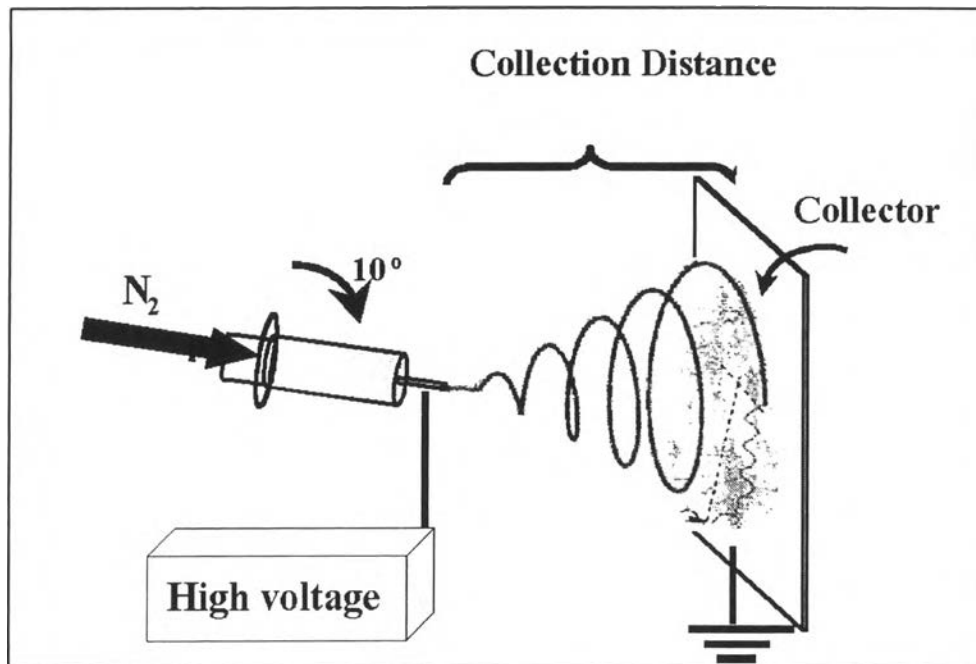


Figure 1

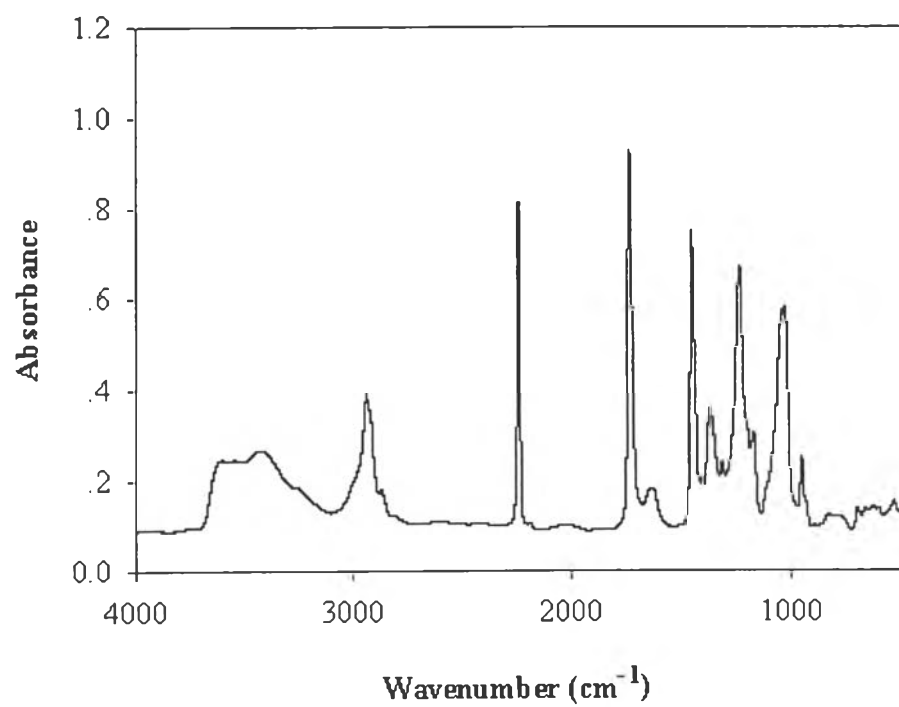
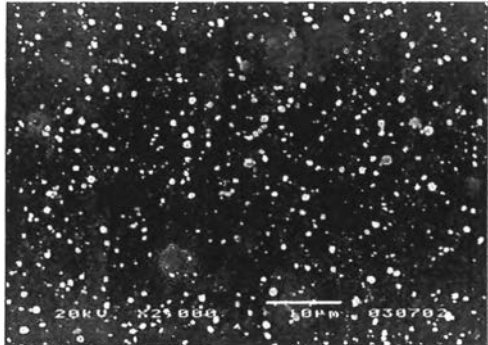
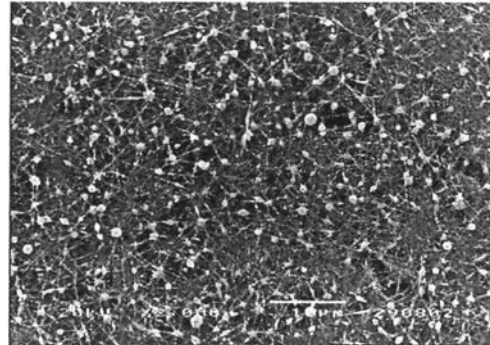


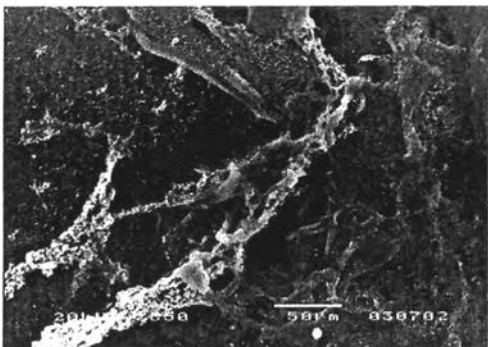
Figure 2



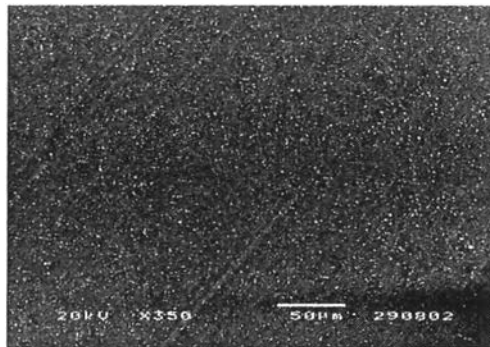
(a) 2.1 wt% (×2,000)



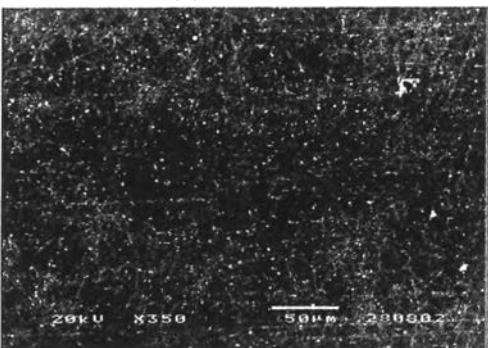
(b) 4.0 wt% (×2,000)



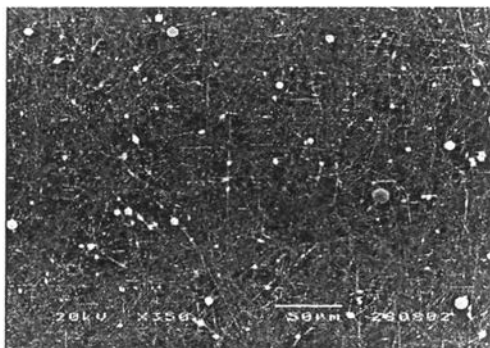
(c) 2.1 wt% (×350)



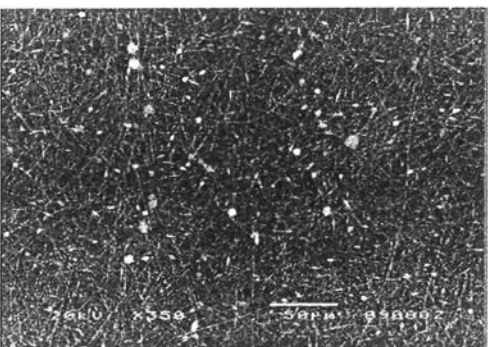
(d) 4.0 wt% (×350)



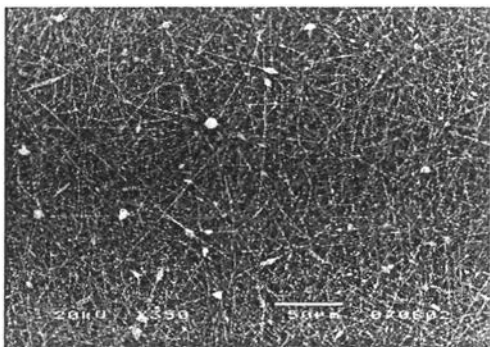
(e) 5.9wt% (×350)



(f) 7.8% (×350)



(g) 9.5 wt% (×350)



(h) 11.2 wt% (×350)

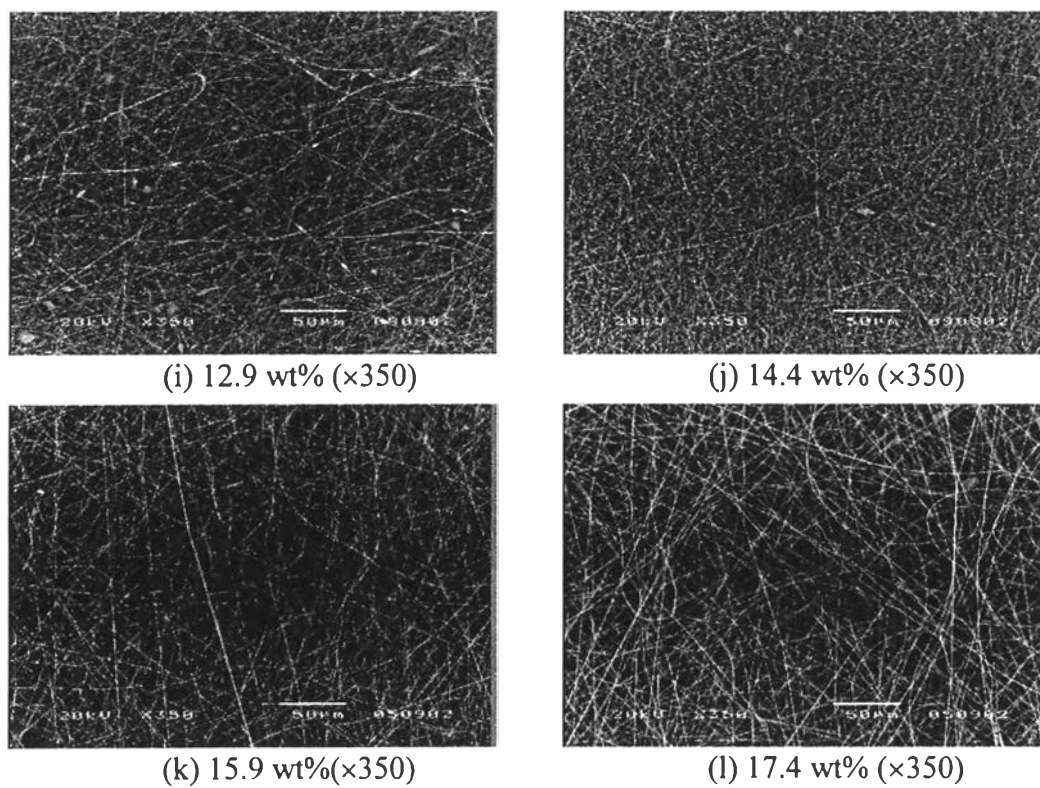


Figure 3

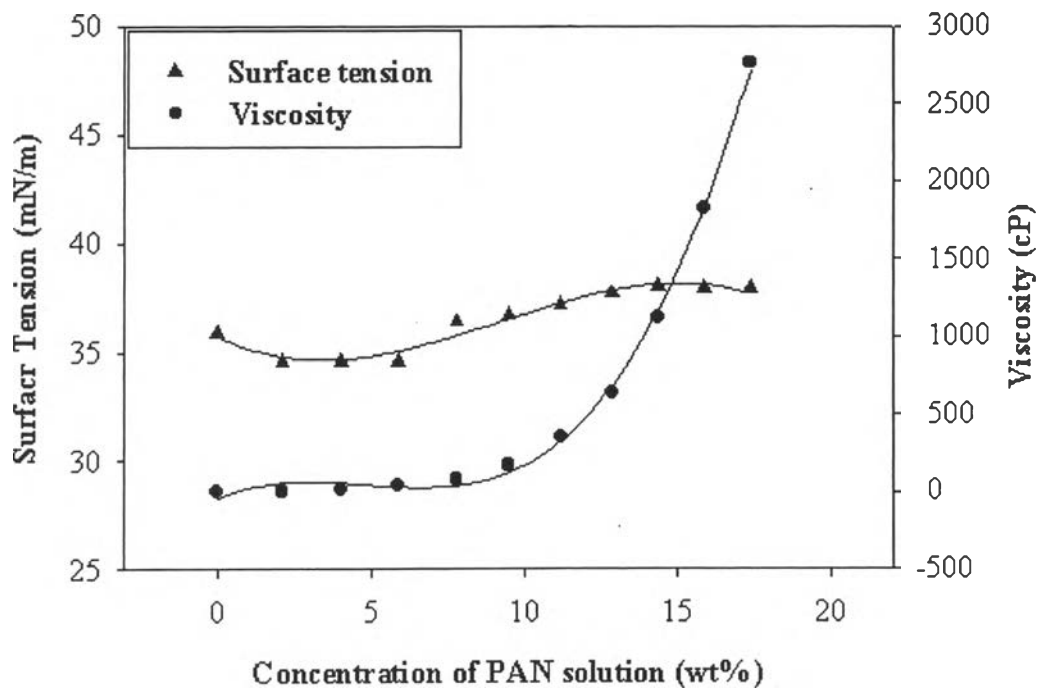


Figure 4

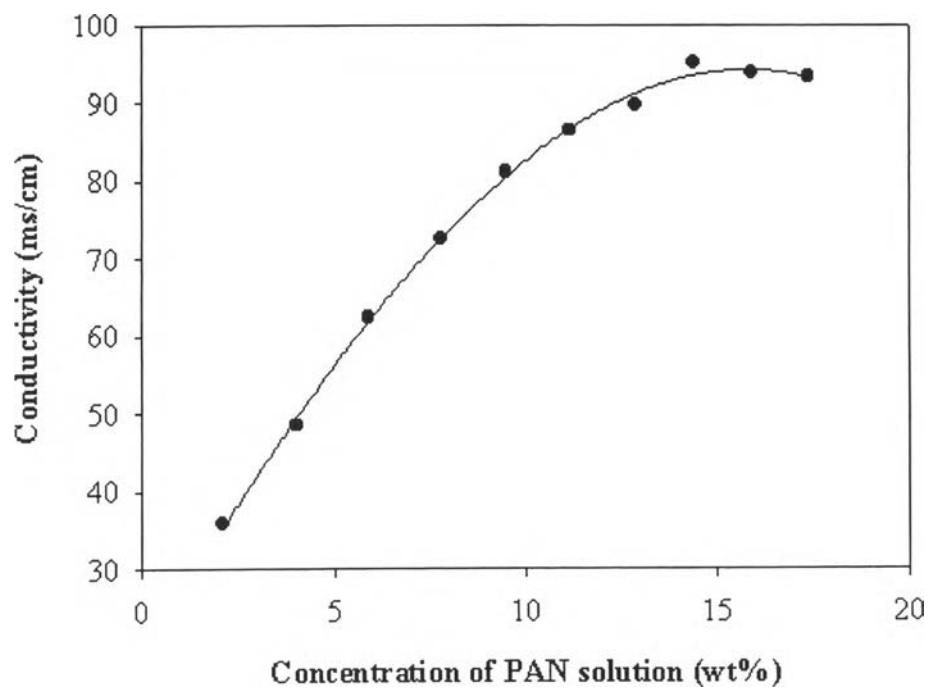


Figure 5

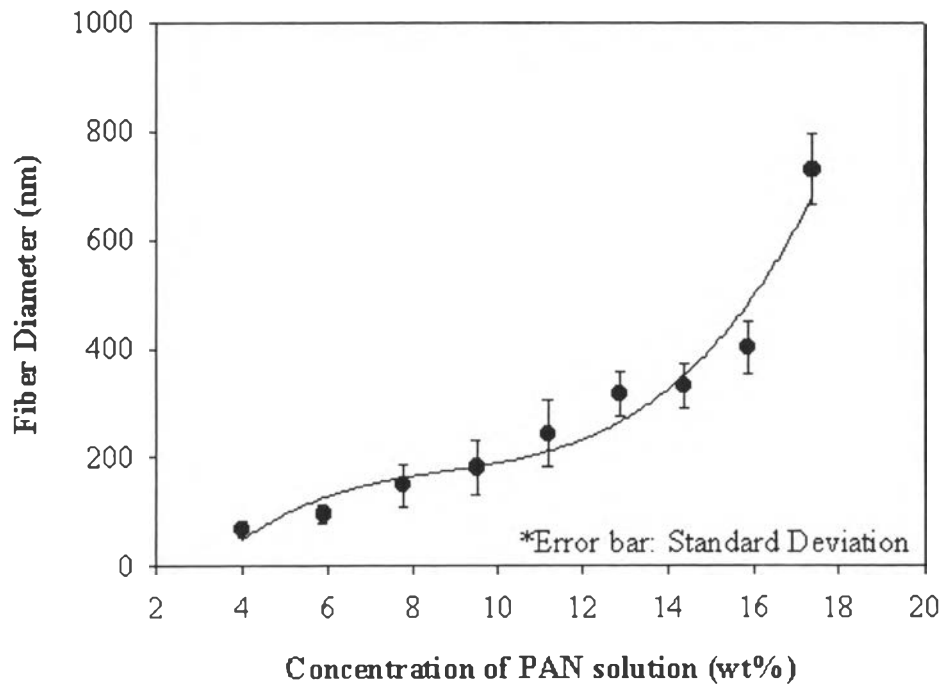


Figure 6

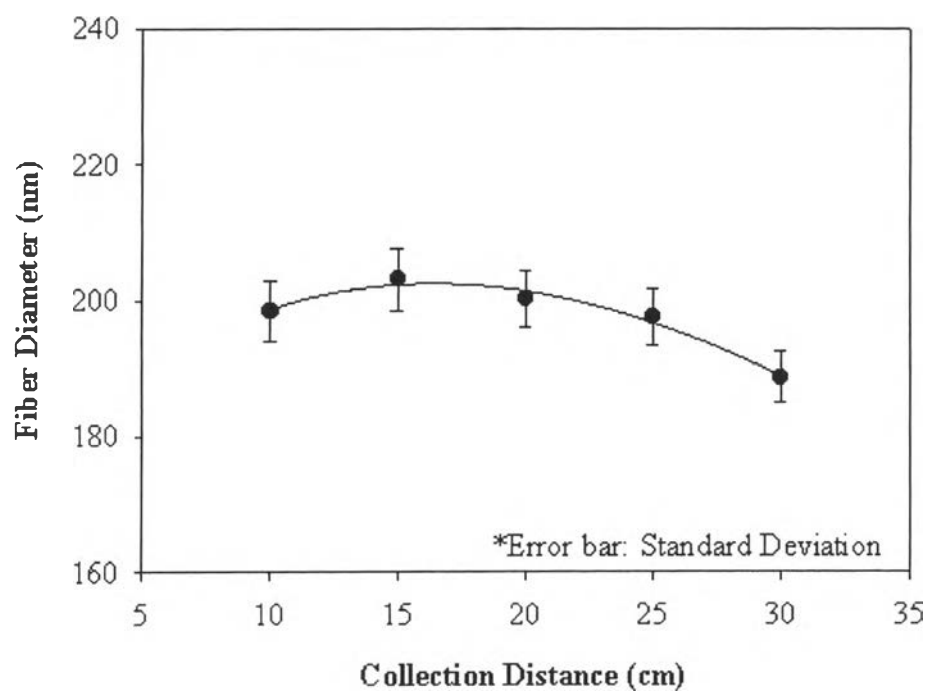
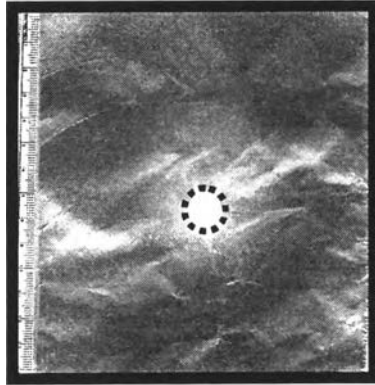
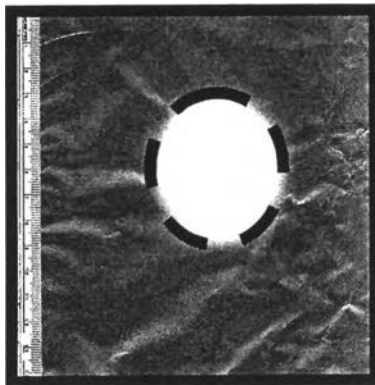


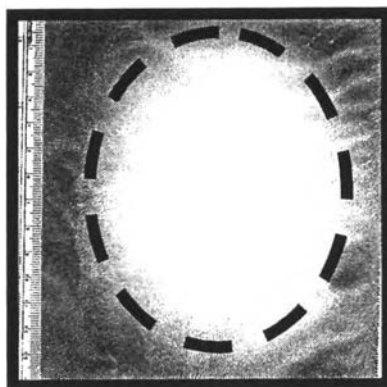
Figure 7



(b) 10 cm



(b) 20 cm



(c) 25 cm

Figure 8

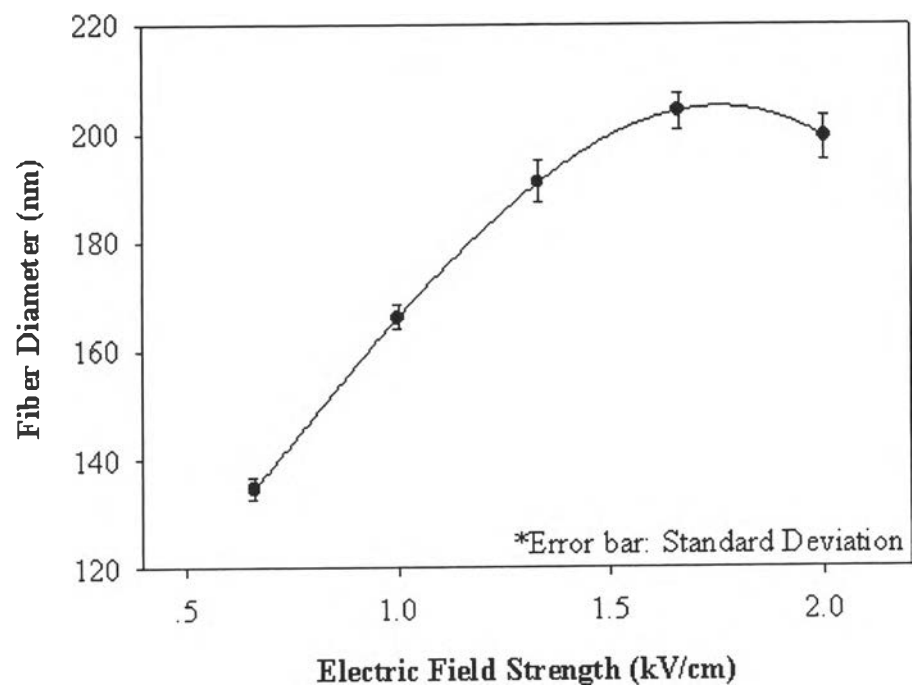


Figure 9

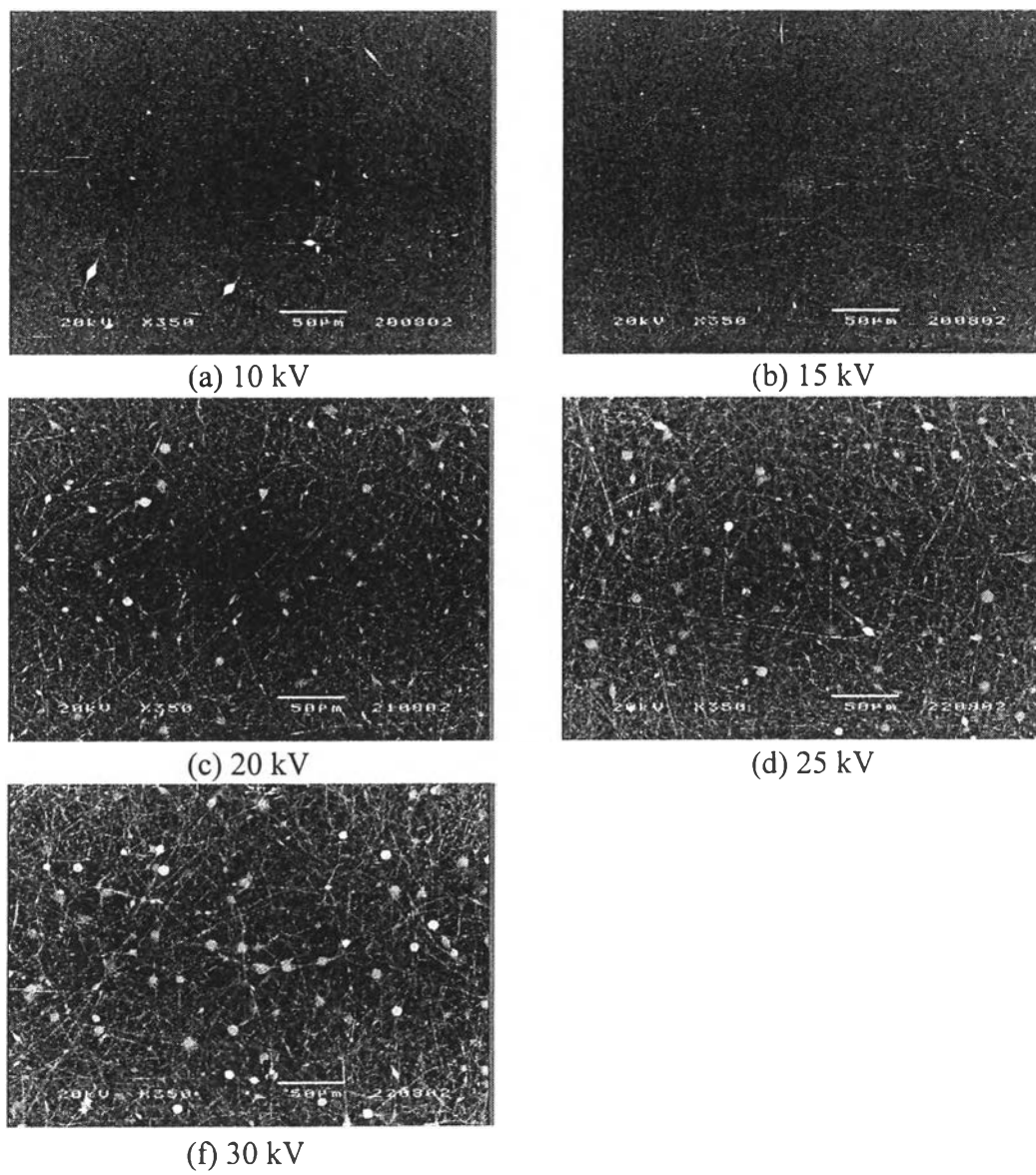


Figure 10

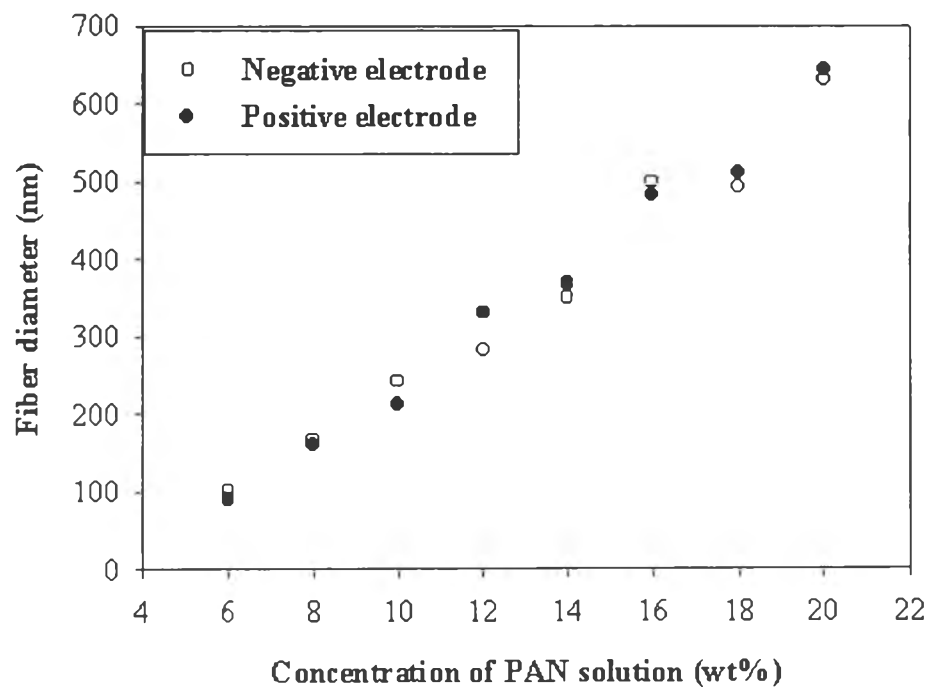


Figure 11

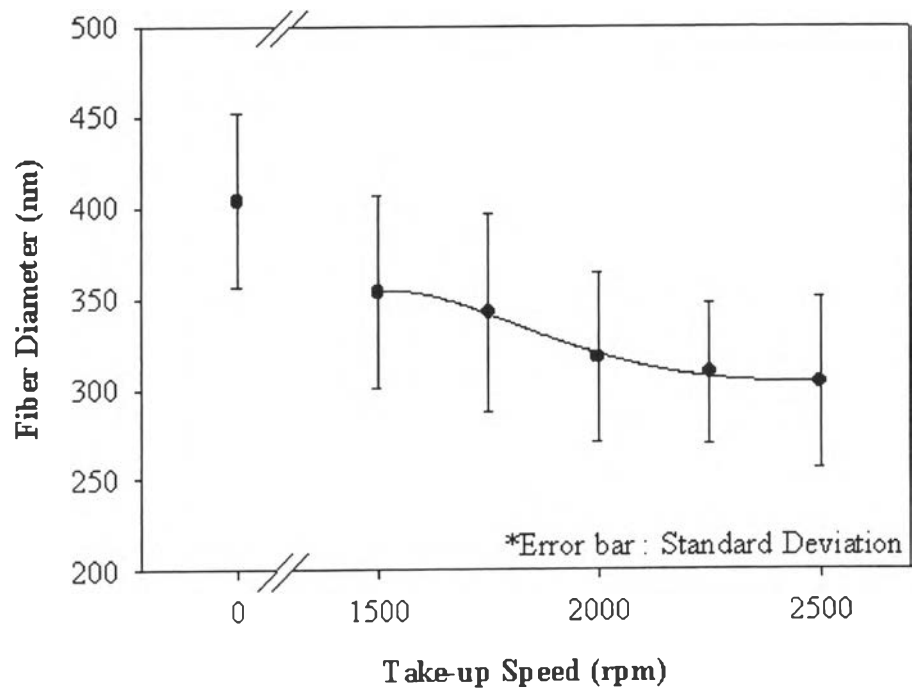


Figure 12

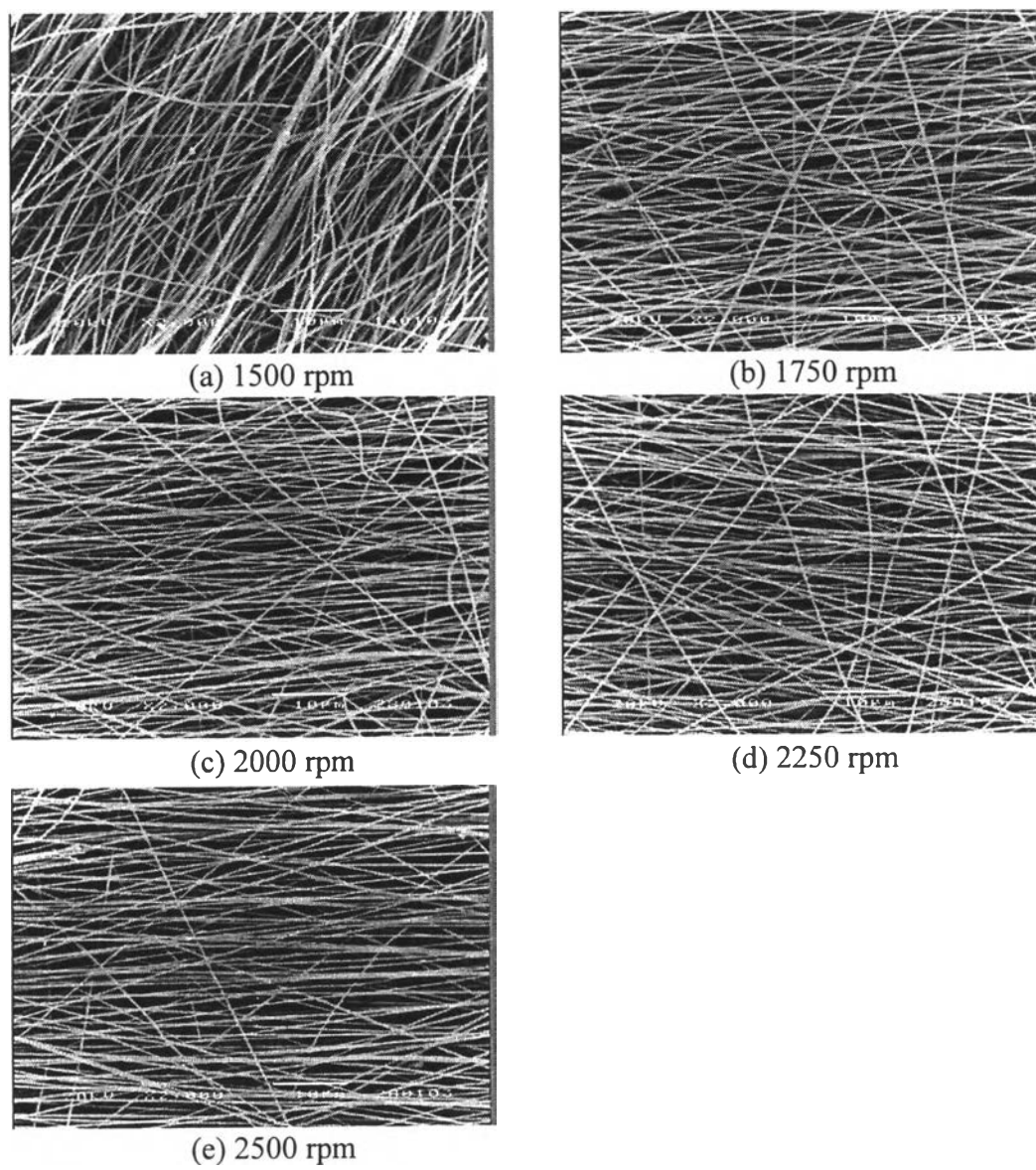


Figure 13

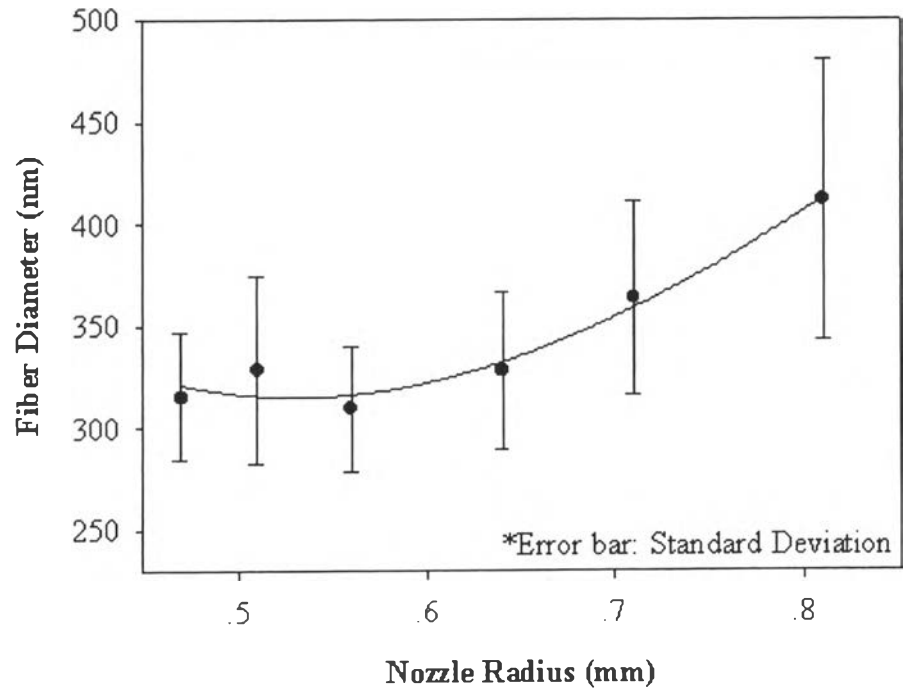
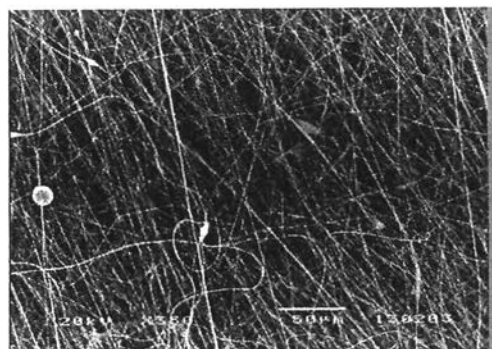
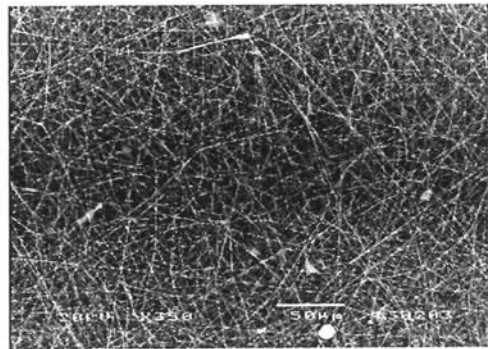


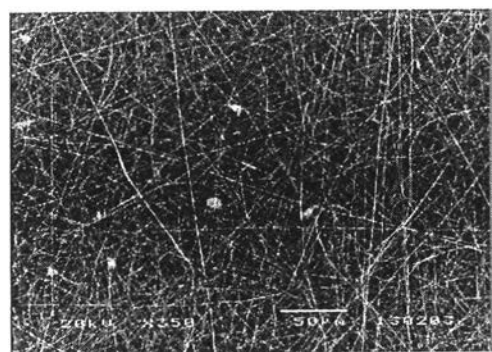
Figure 14



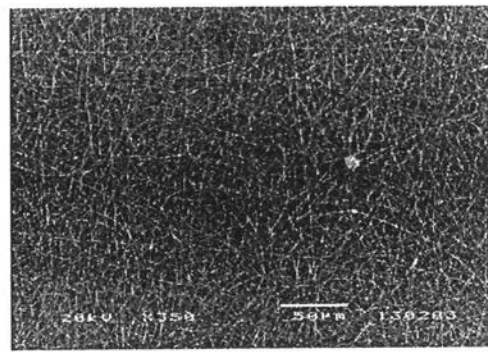
(a) 0.81 mm



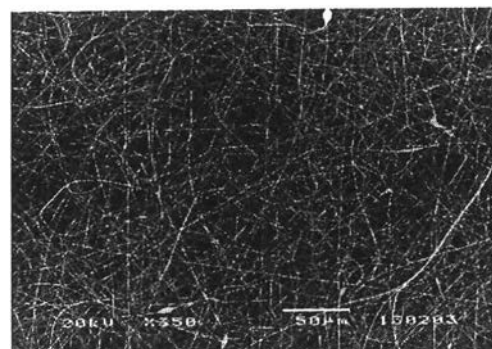
(b) 0.71 mm



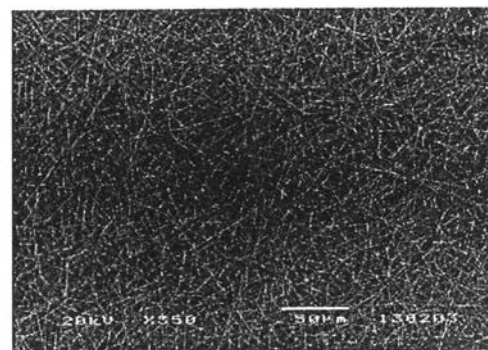
(c) 0.64 mm



(d) 0.56 mm



(e) 0.51 mm



(f) 0.47 mm

Figure 15

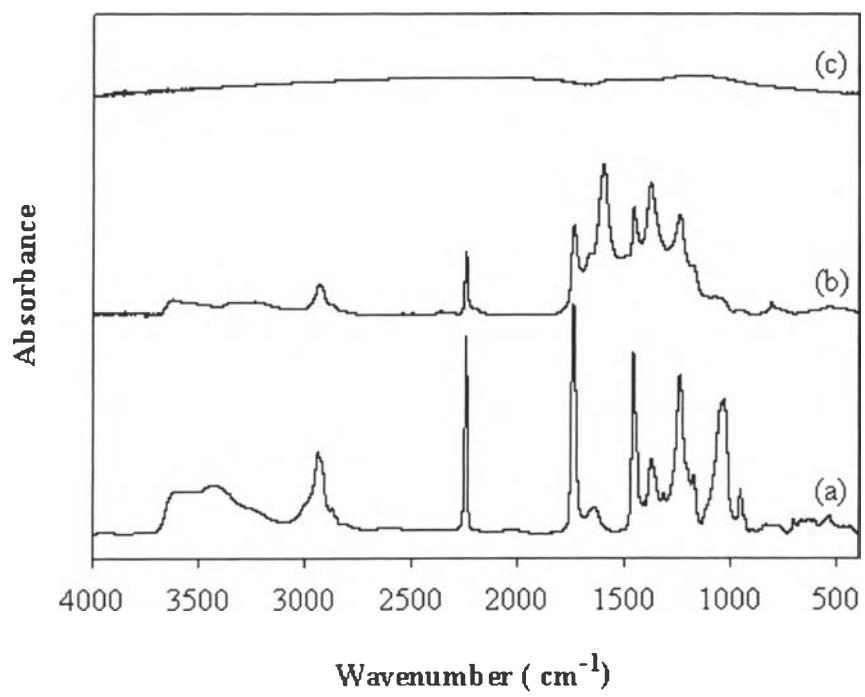


Figure 16

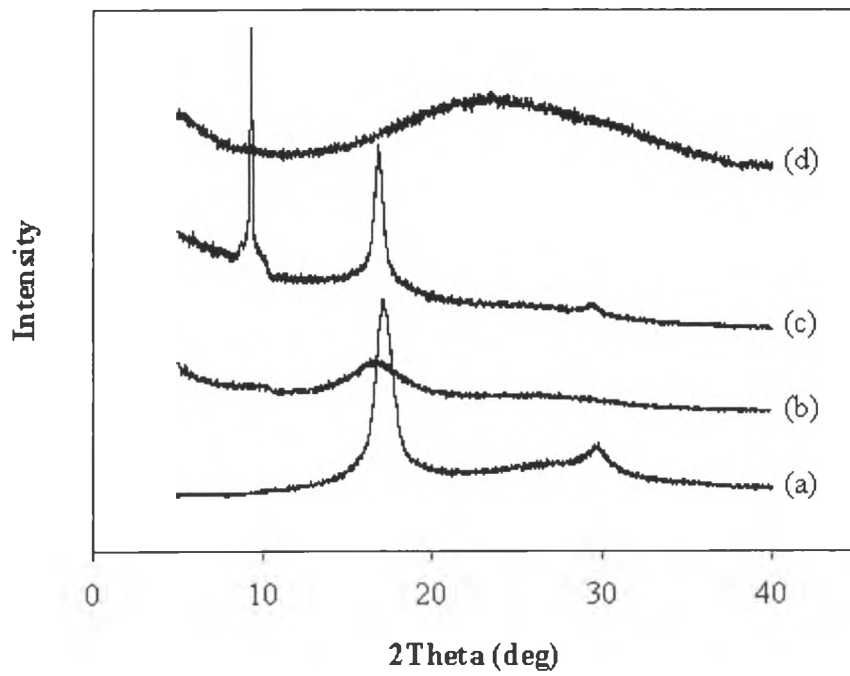


Figure 17

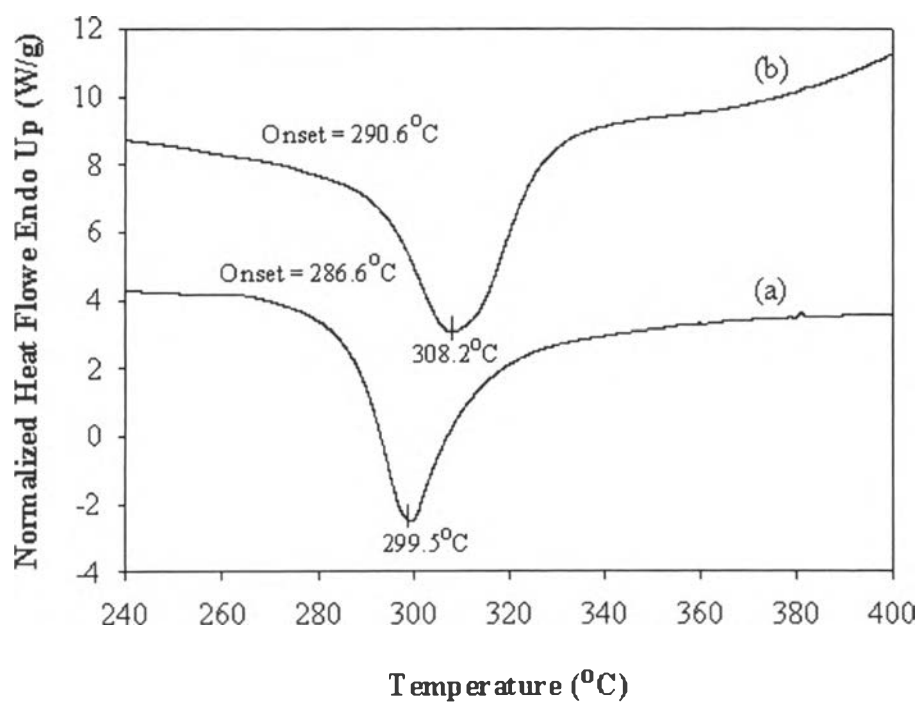


Figure 18

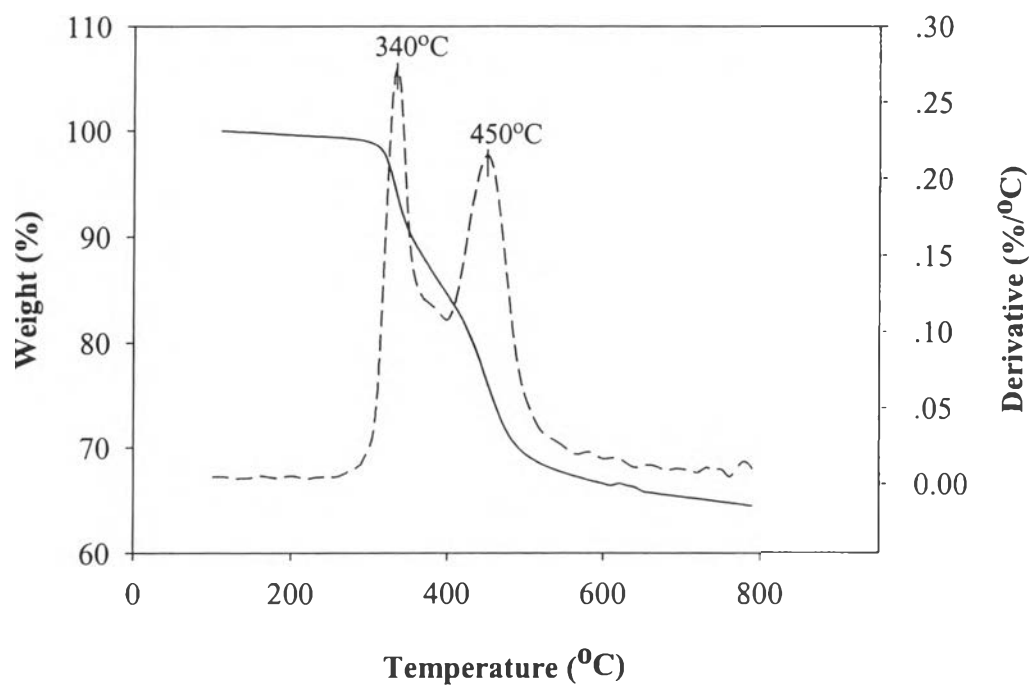


Figure 19

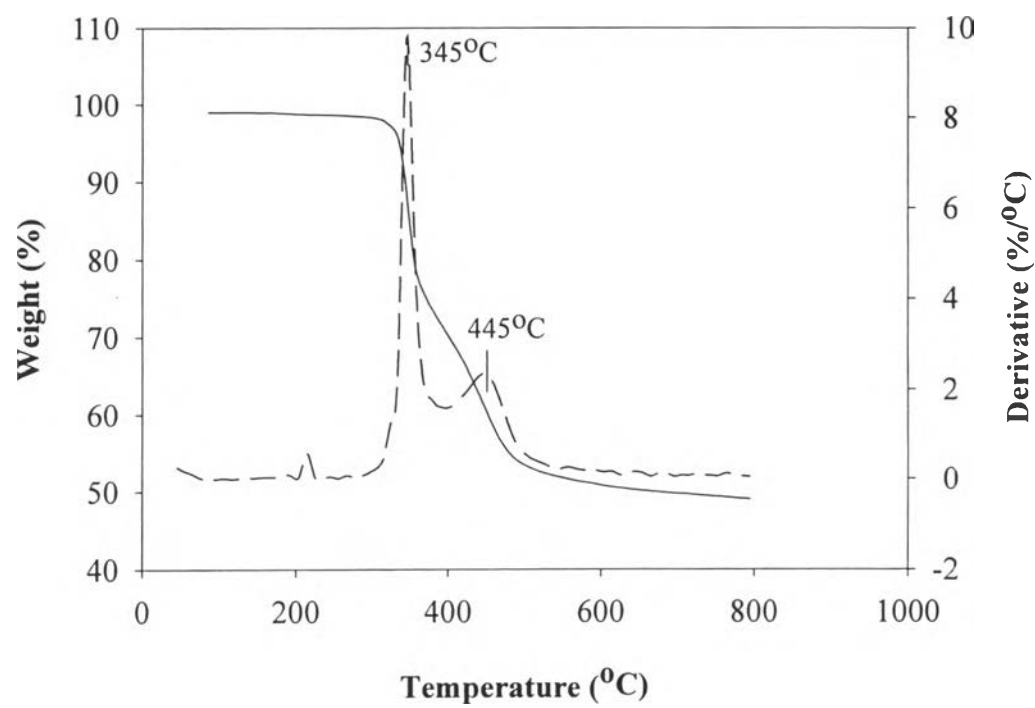


Figure 20

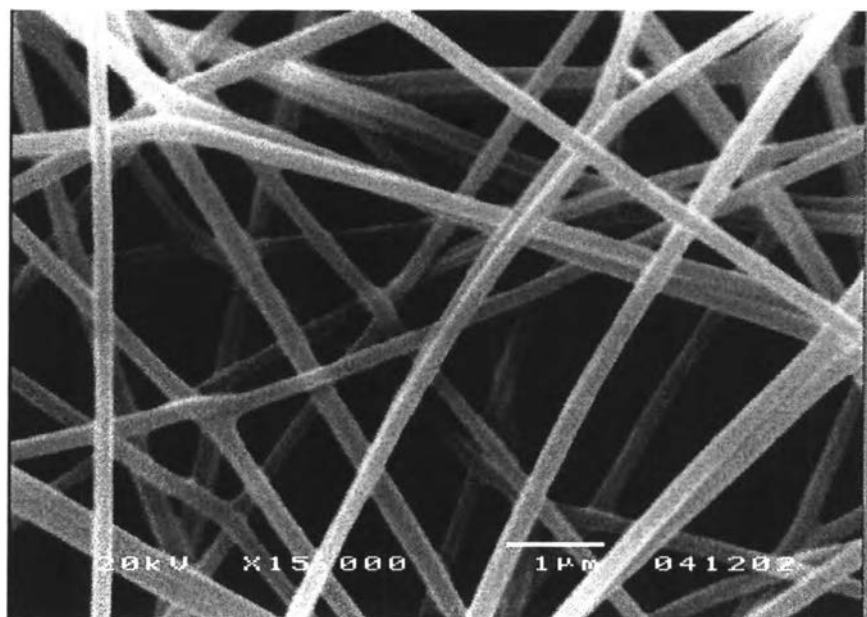


Figure 21